Neoplasma 2025; 72(1–2): 16–24

doi:10.4149/neo_2025_241120N481

Inhibition of enzymatic activity of HRD1 results in death of cells derived from glioblastoma multiforme, neuroblastoma, and normal astrocytes

Jaroslava GUZIKOVA[1], Monika LISKOVA[1], Lubos HUDAK[1], Maria BRODNANOVA[2], Andrea EVINOVA[2], Jozef HATOK[1], Peter RACAY[1,*]

[1]Department of Medical Biochemistry, Comenius University in Bratislava, Jessenius Faculty of Medicine in Martin, Martin, Slovakia; [2]Biomedical Center Martin, Comenius University in Bratislava, Jessenius Faculty of Medicine in Martin, Martin, Slovakia

**Correspondence: peter.racay@uniba.sk*

Received November 20, 2024 / Accepted March 5, 2025

The aim of the present study was to examine the impact of LS-102, an inhibitor of enzymatic activity of HRD1 that is an essential E3 ubiquitin ligase of endoplasmic reticulum associated degradation (ERAD) on survival of the human cell lines derived from glioblastoma multiforme (GBM), neuroblastoma, and astrocytes. We have also examined molecular responses to HRD1 inhibition with a focus on proteins playing an essential role in unfolded protein response (UPR) and ERAD. In addition, activation of IRE1α documented by XBP1 splicing was investigated. Finally, we have examined the impact of LS-102 on p53 expression in GBM cells. Inhibition of HRD1 enzymatic activity results in cell death of all tested cells. With respect to GBM cells, U87 cells are more sensitive to LS-102 as T98G cells. Cells of cell lines derived from normal astrocytes K1884 exhibit the highest sensitivity to LS-102 among all cell types used in the study while NHA cells are the most resistant. Sensitivity of neuroblastoma SH-SY5Y cells to LS-102 is comparable to the sensitivity of U87 cells. In GBM cells, inhibition of HRD1 results in induction of the expression of proteins playing an essential role in UPR and ERAD (HRD1, SEL1L, and GRP78). XBP1 splicing induced by HRD1 inhibition was documented in T98G and K1884 cells. We did not observe induction of p53 expression in U87 cells. Since LS-102 induces cell death of normal astrocytes, it is not a candidate for the testing of its potential use as an antitumor treatment of GBM.

Key words: glioblastoma multiforme; endoplasmic reticulum associated degradation; unfolded protein response; cell death

Glioblastoma multiforme (GBM) is the most common and the most aggressive primary brain tumor [1]. Despite the current treatments, which include surgical resection, chemotherapy using temozolomide and radiotherapy, tumor recurrence occurs in almost all patients resulting in median survival of less than 15 months [2]. GBM diffusely infiltrates the adjacent brain tissue [3] and rarely spreads outside the central nervous system [4]. Diffuse infiltration into the normal brain parenchyma is a hallmark of GBM and underlies recurrence by precluding complete surgical resection [5, 6]. Thus, the development of new therapy of GBM based on cytotoxic drugs represents a great challenge of current biomedical research.

In order to maintain a high proliferation rate, both DNA and protein synthesis are elevated in tumor cells. In addition to deregulated translation, deregulated/overloaded polypeptide processing, including polypeptide modification and folding located in the endoplasmic reticulum (ER) could contribute to the cancer progression [7, 8]. All these factors along with limited oxygen and nutrient supply to the growing tumor [7, 9] result in ER stress and initiation of the unfolded protein response (UPR) [7, 8]. Aberrant folding of proteins in ER and consequent UPR activation, attributed to both intrinsic and extrinsic factors, were documented in many human cancer types [10].

Irrespective of the mechanism of ER stress induction, UPR represents the main response of the cells to ER stress as well as cytoprotective mechanism to cope with stress inducing conditions and to restore ER homeostasis and functions [11]. UPR includes the repression of protein synthesis, the degradation of the unfolded proteins by ER-associated degradation (ERAD) and the promotion of appropriate protein folding mediated by ER chaperones. The expression of ER chaperones depends on the activation of all three arms of UPR signaling that includes activation of the activating transcription factor 6 (ATF6), protein kinase RNA-like ER kinase (PERK), and inositol-requiring enzyme-1α (IRE1α) [11]. ER stress-induced cleavage of ATF6 into an active cytosolic

ATF6 fragment p50 and its consequent translocation to the nucleus activates expression of ER chaperones [12]. Despite significant reduction of overall frequency of mRNA translation initiation resulting from phosphorylation of eIF2α via PERK, ATF4 mRNA is preferentially translated to active ATF4 that also drives the expression of ER chaperones [13]. Finally, the X-box binding protein 1 (XBP1) mRNA cleavage and splicing depends on autophosphorylation of IRE1α that activates IRE1α endoribonuclease. The spliced form of the transcription factor XBP1s induces expression of proteins involved in ERAD [14, 15], ER chaperones and proteins facilitating protein folding [16]. ERAD includes retrotranslocation of aberrant proteins from ER to the cytosol through the membrane spanning retro-translocon [17, 18]. Aberrant proteins are further polyubiquitinated employing E3 ubiquitin ligase HRD1 and finally degraded by the 26S proteasome [18–20]. Activation of IRE1α can also result in cleavage of ER-localized mRNAs in a process known as regulated IRE1α-dependent decay, which further decreases ER translational load and helps to restore cellular homeostasis [21].

Despite induction of cytoprotective UPR, chronic or intensive ER stress can culminate in different forms of cell death [11]. The best described ER stress-induced apoptosis depends on ATF4-mediated expression of CHOP that further initiates expression of pro-apoptotic proteins PUMA and Noxa [11]. Tumor cells, however, exhibit resistance to the different forms of cell death [22]. Previous studies have implicated UPR activation in different aspects of carcinogenesis in a variety of cancer types [7, 8]. A number of small molecules were recently identified to interfere with various arms of the UPR and ERAD, however, potential translation of this knowledge to cancer therapy has been limited to date [23, 24]. The impact of ERAD inhibitor eeyarestatin on either tumor cell survival [25] or chemotherapy sensitivity [26] was examined while the impact of LS-102, an inhibitor of enzymatic activity of HRD1 that represents the central and essential protein of ERAD [19, 20], on cancer cells survival and response was not investigated.

On the basis of previous studies, we assume that the increased rate of protein synthesis in tumor cells leads to an overload of protein quality control mechanisms including ERAD. Since ER stress and consequent UPR signaling in tumor cells could also be increased because of changes in the tumor microenvironment [7, 9] we hypothesize that tumor cells will be more sensitive to ERAD inhibition than normal cells. Thus, in the present study, we have examined the impact of LS-102 on survival of the cells of human cell lines derived from GBM and neuroblastoma. We have used two different glioblastoma cells with opposite characteristics that are important with respect to GBM. T98G cells contain mutant-type *TP53* with positive O^6-methylguanine-DNA methyltransferase (MGMT) that is responsible for the resistance of GBM cells to temozolomide, while U87 cells contain wild-type *TP53* with negative MGMT [27]. In addition, we have investigated the impact of LS-102 on neuroblastoma SH-SY5Y cells and normal human astrocytes represented by NHA and K1884 cells. We have examined molecular responses of the cells to HRD1 inhibition with a focus on expression of proteins playing an essential role in UPR and ERAD as well as on XBP1 splicing. Finally, we have also examined the impact of LS-102 on p53 expression in GBM cells.

Materials and methods

Materials. The following materials were obtained commercially: sodium dodecylsulphate (SDS), bovine serum albumin (BSA), 3-(4,5-dimethylthiazol-2-yl)-2,5-diphenyltetrazolium bromide (MTT), trypsin (EC 3.4.21.4), 3-[(3-cholamidopropyl)dimethylammonio]-1-propanesulfonate hydrate (CHAPS) (AppliChem GmBH, Germany); tunicamycin (Calbiochem, Germany); LS-102 (Merck, NJ, USA); HALT™ protease inhibitor cocktail (Thermo Fisher Scientific, MA, USA); prestained protein standards (#1610373, BioRad, CA, USA); mouse monoclonal antibodies against HSP60 (#SC-271215, Santa Cruz Biotechnology, Germany), p53 (#SC-55476, Santa Cruz Biotechnology) and β-actin (#3700, Cell Signaling, MA, USA); rabbit polyclonal antibody against HRD1 (#13473-1-AP, Proteintech, IL, USA); GRP78 (#ab227865, Abcam, UK); SEL1L (#PA5-88333, Invitrogen, CA, USA); LONP1 (#PA5-51692, Invitrogen); goat anti-rabbit (#A0545, Sigma-Aldrich, MO, USA) and goat anti-mouse (#A0168, Sigma-Aldrich) secondary antibodies conjugated with horse radish peroxidase.

Cell culture and treatment. Glioblastoma U87 cells (ATCC, VA, USA) were maintained in DMEM medium (Thermo Fisher Scientific) supplemented with 10% fetal bovine serum and 1% penicillin-streptomycin (all PAA, Austria) at 37 °C and 5% CO_2 humidified atmosphere.

Glioblastoma T98G cells (ATCC) were maintained in DMEM medium (Thermo Fisher Scientific) supplemented with 10% fetal bovine serum and 1% penicillin-streptomycin (all PAA) at 37 °C and 5% CO_2 humidified atmosphere.

Primary human astrocytes K1884 (Gibco, CA, USA) were maintained in a specific medium for astrocyte growth (DMEM 1×, GlutaMAX, N-2 Supplement, One Shot FBS) (Thermo Fisher Scientific) at 37 °C and 5% CO_2 humidified atmosphere.

Primary human astrocytes NHA (ATCC) were maintained in MEM medium (Thermo Fisher Scientific) medium supplemented with 10% fetal bovine serum and 1% penicillin-streptomycin (all PAA) at 37 °C and 5% CO_2 humidified atmosphere.

Neuroblastoma SH-SY5Y cells (ATCC) were maintained in DMEM:F12 (1:1) medium supplemented with 10% fetal bovine serum and 1% penicillin-streptomycin (all PAA) at 37 °C and under a 5% CO_2 humidified atmosphere.

The media were changed every 3 days.

The cells were treated with the indicated concentrations of LS-102 for 24 h at 37 °C and under a 5% CO_2 humidified

atmosphere. At the end of the treatment, the cells were washed 3 times with ice-cold phosphate-buffered saline (PBS) and then re-suspended in a lysis buffer (30 mmol/l Tris-HCl, 150 mmol/l NaCl, 1% CHAPS, 1× protease inhibitor cocktail, pH 7.6) for total protein extraction. Protein concentrations were determined by a protein DC assay kit (Bio-Rad, CA, USA) with BSA as a standard.

Cell viability. The cells were seeded in 96-well plates at optimal concentrations. Control cells and the cells treated with LS-102 were incubated for indicated time intervals at 37 °C under a 5% CO_2 humidified atmosphere. At the end of incubation, a 0.01 ml MTT solution (5 mg/ml) was added to each well, and the cells were further incubated for 4 hours at 37 °C and under a 5% CO_2 humidified atmosphere. The insoluble formazan, which resulted from the oxidation of added MTT by vital cells, was dissolved by the addition of 0.1 ml of SDS solution (0.1 g/ml) and overnight incubation at 37 °C under a 5% CO_2 humidified atmosphere. The absorbance of formazan was determined spectrophotometrically by using a Synergy H4 microplate reader (Agilent, CA, USA). The relative viability of the cells was determined as the ratio of the optical density of formazan produced by treated cells to the optical density of the formazan produced by untreated control cells and was expressed as a percentage of the control. For each treatment time, the optical density value of untreated control cells was considered as 100% of viable cells.

Western blotting (WB). Isolated proteins (30 μg proteins loaded/lane) were separated on 10% SDS-polyacrylamide gel electrophoresis (PAGE) under reducing conditions. Separated proteins were transferred to nitrocellulose membranes by using semi-dry transfer, and membranes were probed with antibodies specific to GRP78 (1:1000), HRD1 (1:1000), HSP60 (1:1000), LONP1 (1:1000), SEL1L (1:1000), p53 (1:1000), and β-actin (1:2000). Further incubation of the membranes with particular secondary antibodies (1:10000 mouse, 1:20000 rabbit) was followed by the visualization of immunopositive bands by using the chemiluminescent substrate SuperSignal West Pico (Thermo Fisher Scientific) and the Chemidoc XRS system (Bio-Rad). Intensities of specific bands were quantified by Quantity One software (Bio-Rad). The intensities of bands of interest were normalized to corresponding intensities of bands of β-actin and were expressed as the intensity of the band of the particular protein in treated cells relative to the intensity of the band in control untreated cells.

Isolation of total RNA and cDNA synthesis. Total RNA was isolated from harvested cells treated with the indicated concentrations of either LS-102 or tunicamycin at a concentration 2 μmol/l for 6 h at 37 °C using Tri reagent (MRC) following the manufacturer's protocol. Total RNA (1 μg) was reversely transcribed to cDNA by using a mRNA-MAXIMA First Strand cDNA synthesis kit (Thermo Fisher Scientific) according to the protocol supplied by the manufacturer.

Reverse-transcription polymerase chain reaction (RT-PCR). Aliquots of the resulting cDNA corresponding to 5 ng total RNA were used for PCR. Sequences of primers used for amplification of XBP1 mRNA (Table 1) were designed and verified by using the nucleotide database of the National Center for Biotechnology Information. Amplification of the cDNAs was initiated by denaturation at 95 °C for 3 min, followed by 35 PCR cycles (initial denaturation at 95 °C for 3 min followed by cycles of denaturation at 95 °C for 30 s, annealing at 58 °C for 30 s, and extension at 72 °C for 30 s) and final extension at 72 °C for 7 min in a DNA thermal cycler (Biometra). The PCR products were separated by electrophoresis in 3% agarose gel and then visualized by ethidium bromide staining.

Table 1. Sequences of oligonucleotides used as primers for RT-PCR.

Gene	Forward primer	Reverse primer
XBP1	CCTGGTTGCTGAAGAGGAGG	CCATGGGGAGATGTTCTGGA

Statistical analysis. One-way ANOVA (GraphPad InStat V2.04a, GraphPad Software) was first carried out to test for differences among all experimental groups. Additionally, Tukey's test was used to determine the differences between individual groups. A p-value <0.05 was considered as being significant.

Results

Impact of LS-102 on relative cell viability of the cells. The testing of the relative cell viability with the MTT assay at 24, 48, and 72 h after the treatment of the cells with different concentrations of LS-102 revealed a concentration-dependent reduction of the relative viability of the cells of the investigated cell lines (Figure 1). The IC50 values (concentrations causing decrease of the relative cell viability to 50% of the control untreated cells) for the used cell lines are summarized in Table 2. As indicated, the cells of astrocyte cell line K1884 exhibit the highest sensitivity while the cells of glioblastoma cell line T98G are the most resistant (Table 2). The kinetics of the cell death seem to be fast. Although there is a trend towards decreased IC50 values with an increased time of treatment, the time-dependent changes of IC50 values are not statistically significant.

Impact of LS-102 on expression of proteins involved in UPR and ERAD. In order to test the impact of LS-102 on expression of proteins involved in UPR and ERAD, we have performed the western blot analysis of the protein extracts prepared from control untreated cells and the cells treated with indicated concentrations of LS-102 for 24 h. We have focused on GRP78, which is the master protein involved in activation of UPR [11], and HRD1, which is an E3 ligase involved in ERAD [18]. Interaction of HRD1 with SEL1L is a prerequisite for the formation of a functional HRD1-ERAD complex [28], therefore we have also analyzed the impact of LS-102 on the expression of SEL1L. Since HRD1 is also involved in regulation of mitochondrial biogenesis [29] and dynamics [30], we have also examined the impact of LS-102

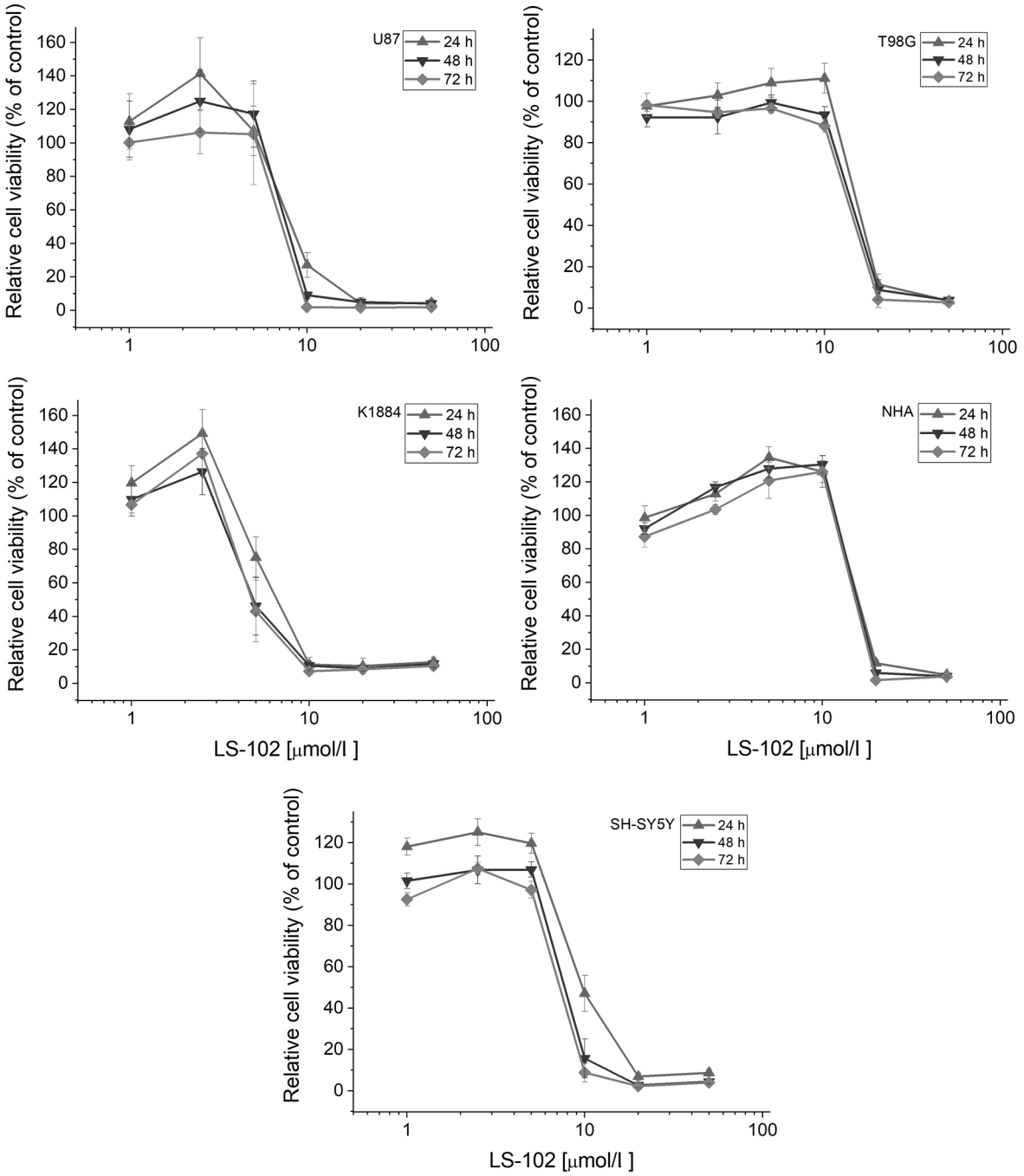

Figure 1. Impact of LS-102 on relative cell viability. U87, T98G, K1884, NHA, and SH-SY5Y cells were treated with the indicated concentrations of LS-102 for 24, 48, and 72h, and then the relative viability was determined by MTT test as described in Materials and methods. Data are presented as means ± SEM (4 independent experiments performed in triplicate per each treatment).

on the levels of HSP60 and LONP1 that are important molecular components of mitochondrial UPR [31].

Treatment of the T98G cells for 24 h with LS-102 at a concentration 10 μmol/l (Figure 2) was associated with significant increase of expression of HRD1 (202.3% of control, $p<0.01$), GRP78 (226.1% of control, $p<0.01$), and SEL1L (187.4% of control, $p<0.01$). After the treatment of the T98G cells for 24 h with LS-102 at a concentration 5 μmol/l, the levels of HRD1, GRP78, and SEL1L were elevated but the changes were not statistically significant (Figure 2). The levels of HSP60 and LONP1 were not significantly changed at both investigated concentrations (Figure 2).

The similar results were observed after the treatment of U87 cells with LS-102 (Figure 3). We have observed significantly increased levels of HRD1 (194.3% of control, p<0.01), GRP78 (228.3% of control, p<0.01), and SEL1L (216.9% of control, p<0.01) after the treatment of the U87 cells for 24 h with LS-102 at a concentration 5 μmol/l while the levels of HRD1, GRP78, and SEL1L were not significantly increased after the treatment of the U87 cells for 24 h with LS-102 at a concentration 2.5 μmol/l (Figure 3). The levels of HSP60 and LONP1 were not significantly changed at both investigated concentrations (Figure 3).

The levels of all studied proteins were not significantly changed after the treatment of both SH-SY5Y (Figure 4) and K1884 (Figure 4) cells for 24 h with indicated concentrations of LS-102.

Impact of LS-102 on splicing of XBP1 mRNA. In order to test the impact of LS-102 on activation of IRE1α-XBP1 axis of UPR, we have treated the cells with different concentrations of LS-102 followed with RT-PCR analysis of RNA isolated from control untreated cells and cells treated with LS-102 for 6 h. The time interval was selected on the basis of our previous publications [15, 32]. In addition, RNA isolated from the cells treated with tunicamycin at a concentration of 2 μmol/l for 6 h has also been analyzed serving as a positive control. In agreement with our previous studies [15, 32], treatment of all cells with tunicamycin was associated with splicing of XBP1 mRNA (Figure 5). Treatment of the cells with LS-102 induced splicing of XBP1 mRNA in T98G and K1884 cells while the splicing of XBP1 mRNA was not observed after the treatment of SH-SY5Y and U87 cells with indicated concentrations of LS-102 (Figure 5).

Impact of LS-102 on p53 expression in glioblastoma cells. In order to explain differential sensitivity of GBM cells to LS-102, we have performed WB analysis of p53 expression in U87 and T98G cells since it was documented earlier that HRD1 targets p53 for ubiquitination and further destruction [33]. In accordance with a generally accepted view that mutant p53 is stable, we have documented significantly stronger signal of p53 in T98G cells as compared to the signal of p53 in U87 cells (Figure 6). Treatment of U87 cells with LS-102 was not associated with elevated expression of p53 (Figure 6). In addition, treatment of U87 cells with LS-102 was not associated with activation of caspase 3 (Supplementary Figure S1).

Table 2. IC50 values of LS-102 for different cell lines.

	IC50 (μmol/l)		
	24 h	48 h	72 h
SH-SY5Y	9.81±0.85	8.20±0.49	7.68±0.12
T98G	16.12±0.91	15.15±0.86	14.55±0.73
U87	8.51±0.81	8.05±0.34	7.55±0.71
NHA	16.59±0.62	16.45±0.35	16.08±0.43
K1884	6.61±1.32	5.18±1.61	5.14±1.72

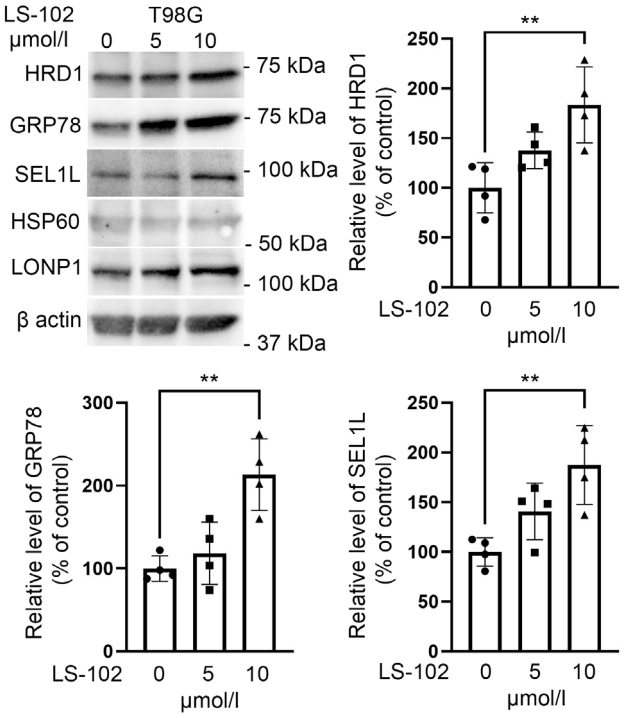

Figure 2. Impact of LS-102 on expression of HRD1, GRP78, SEL1L, HSP60, and LONP1 in T98G cells. Total cell extracts were prepared from T98G cells after treatment with LS-102 at concentrations 5 and 10 μM. The effect of the treatment on the levels of HRD1, GRP78, SEL1L, HSP60, and LONP1 was evaluated by the western blot analysis of total cell extracts as described in Materials and methods. β-actin served as the loading control. The representative blots are cropped from different parts of the same blot. The levels of HRD1, GRP78, and SEL1L were normalized to β-actin levels and expressed as relative to untreated controls. Data are presented as means ± SD (4 independent experiments per each treatment). **p<0.01 (one-way ANOVA, followed by Tukey's test to determine differences between the protein levels in control untreated cells and treated cells).

Discussion

In this study, we have documented the sensitivity of different cell types derived from GBM, neuroblastoma, and normal astrocytes to the inhibitor of HRD1 enzymatic activity LS-102. With respect to GBM cells, U87 cells are very sensitive to LS-102 while T98G cells are less sensitive to the inhibition of HRD1 function. Cell lines derived from normal astrocytes exhibit also differential sensitivity to LS-102. K1884 cells exhibit the highest sensitivity to LS-102 among all cell types used in the study, while NHA cells are the most resistant. Sensitivity of neuroblastoma SH-SY5Y cells to LS-102 is comparable to the sensitivity of U87 cells. In addition, we have shown that inhibition of HRD1 has differential impact on induction of expression of HRD1, SEL1L, and GRP78 as well as on XBP1 mRNA splicing.

HRD1 is ER resident E3 ligase playing an essential role in the process of ERAD [17, 18] that is an important mecha-

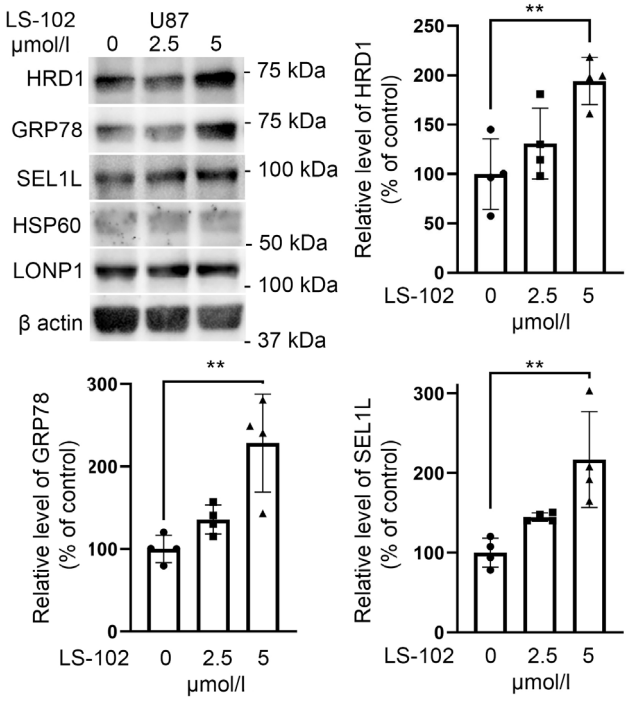

Figure 3. Impact of LS-102 on expression of HRD1, GRP78, SEL1L, HSP60, and LONP1 in U87 cells. Total cell extracts were prepared from U87 cells after treatment with LS-102 at a concentration of 2.5 and 5 μmol/l. The effect of the treatment on the levels of HRD1, GRP78, SEL1L, HSP60, and LONP1 was evaluated by the western blot analysis of total cell extracts as described in Materials and Methods. β-actin served as the loading control. The representative blots are cropped from different parts of the same blot. The levels of HRD1, GRP78, and SEL1L were normalized to β-actin levels and expressed as relative to untreated controls. Data are presented as means ± SD (4 independent experiments per each treatment). **p<0.01 (one-way ANOVA, followed by Tukey's test to determine differences between the protein levels in control untreated cells and treated cells).

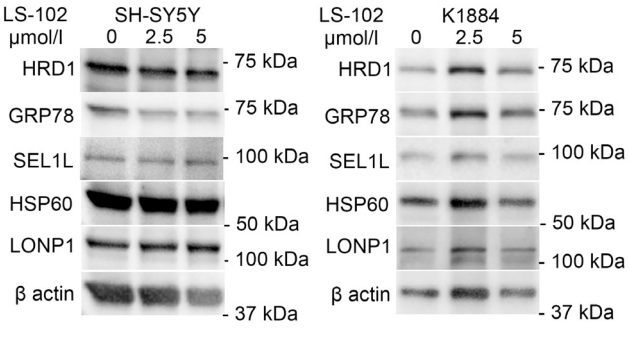

Figure 4. Impact of LS-102 on expression of HRD1, GRP78, SEL1L, HSP60, and LONP1 in SH-SY5Y and K1884 cells. Total cell extracts were prepared from SH-SY5Y and K1884 cells after treatment with LS-102 at concentrations 2.5 and 5 μmol/l. The effect of the treatment on the levels of HRD1, GRP78, SEL1L, HSP60, and LONP1 was evaluated by the western blot analysis of total cell extracts as described in Materials and methods. β-actin served as the loading control. The representative blots are cropped from different parts of the same blot.

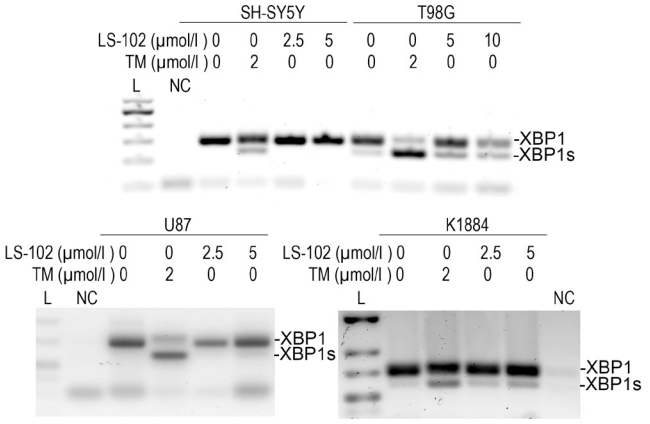

Figure 5. Impact of LS-102 on XBP1 splicing. Total RNA was isolated from T98G, SH-SY5Y, U87, and K1884 cells treated with indicated concentrations of LS-102 or tunicamycin (TM) at a concentration 2 μmol/l for 6 h. XBP1 splicing was evaluated by RT-PCR followed by agarose gel electrophoresis as described in Materials and methods. L-ladder, NC-negative control, no cDNA added in reaction mixture.

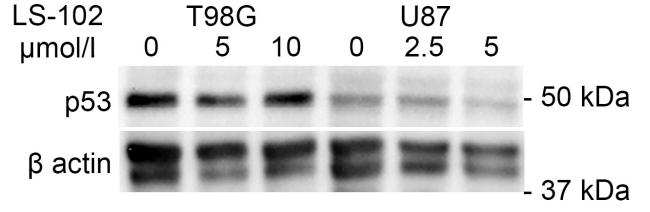

Figure 6. Impact of LS-102 on p53 expression in glioblastoma cells. Total cell extracts were prepared from T98G and U87 cells after treatment with indicated concentrations of LS-102. The effect of the treatment on the level of p53 was evaluated by the western blot analysis of total cell extracts as described in Materials and methods. β-actin served as the loading control. The representative blots are cropped from different parts of the same blot.

nism of the quality control of secretory pathway proteins. Inhibitors of HRD1 were designed as novel candidates for the treatment of rheumatoid arthritis [34] but their effectiveness to kill malignant cells is less described [23]. In our previous study, we have shown that expression of HRD1 depends on ribonuclease activity of IRE1α that results in splicing of XBP1 mRNA [15]. In glioblastoma cells T98G and U87, the inhibition of HRD1 activity was associated with increased expression of HRD1, SEL1L, and GRP78. While in T98G cells increased expression of HRD1 after the treatment of the cells with LS-102 correlates well with the activation of IRE1α documented by XBP1 splicing, the expression of HRD1 after treatment of both U87 and K1884 cells with LS-102 does not correlate with activation of IRE1α. In U87 cells, inhibition of HRD1 resulted in increased expression of HRD1 but was not associated with splicing of XBP1. On the contrary, inhibition of HRD1 does not result in increased expression of HRD1 in K1884 cells

despite documented splicing of XBP1. Thus, the results presented in this study do not indicate the sole relationship between IRE1α activity and expression of HRD1. It seems that the relationship between HRD1 activity and expression of either GRP78 or SEL1L is even more complex. In response to ER stress, upregulation of SEL1L involves activation of the ATF6 branch of UPR, while the expression of HRD1 depends on activation of IRE1-dependent splicing of XBP1 [15]. With respect to ERAD, the recent study documented that downregulation of HRD1 was associated with increased expression of SEL1L in the cells of macrophage cell line RAW 264.7 [35]. These results and results presented in our study indicate a possible association between HRD1 activity/level and expression of SEL1L. On the contrary, downregulation of SEL1L resulted in decreased expression of HRD1 in both HEK239T cells [28] and bone marrow-derived macrophages of myeloid cell-specific *Sel1L*-deficient mice [35]. Interestingly, expression of GRP78 in bone marrow-derived macrophages of myeloid cell-specific *Sel1L*-deficient mice was increased [35]. In response to ER stress, expression of GRP78 is regulated by PERK-ATF4 branch of UPR [36]. The previously published results together with results of our study indicate that the regulation of expression of critical molecular components of both UPR and ERAD is more complex and cell specific, but the mechanism of increased expression of HRD1, GRP78, and SEL1L after inhibition of HRD1 is unclear. Increased expression of GRP78 correlates well with tumor characteristics and was documented in GBM upon recurrence [37]. Overexpression of both HRD1 and GRP78 is considered to be cytoprotective [38] or associated with aggressive growth and invasive properties of cancer cells [39]. In GBM cells, it might represent a compensatory intracellular mechanism to cope with HRD1 inhibition and should confer some resistance to cell death. Despite similar molecular responses of both T98G and U87 cells to the inhibition of HRD1, the sensitivity of the GBM cells to LS-102 was significantly different. Differential sensitivity of GBM cells to LS-102 might also be attributed to the fact that resistant T98G cells are expressing a mutant form of p53, while sensitive U87 cells are expressing wild type of p53 [27]. It was documented earlier that HRD1 targets p53 for ubiquitination and further destruction [33]. Since we did not observe induction of p53 in U87 cells treated with LS-102, we presume that p53-dependent apoptosis is not a mechanism of death of GBM cells induced by LS-102. Thus, the mechanism of differential sensitivity of GBM cells to LS-102 is not clear but it is not dependent on cellular status of *TP53* gene and p53-induced apoptosis.

In conclusion, we have shown that inhibition of HRD1 enzymatic activity by micromolar concentrations of LS-102 is associated with a fast death of the cells of all cell lines used in the study. The impact of LS-102 on XBP1 splicing and expression of HRD1, SEL1L, and GRP78 was specific to GBM cells but does not correlate with sensitivity of the cells to LS-102. Since LS-102 induces also death of normal astrocytes, it is not a candidate for the testing of its potential use as a treatment of GBM.

Supplementary information is available in the online version of the paper.

Acknowledgments: This work was supported by the Scientific Grant Agency under contract no. VEGA 1/0183/23.

References

[1] DAVIS ME. Epidemiology and Overview of Gliomas. Semin Oncol Nurs 2018; 34: 420–429. https://doi.org/10.1016/j.soncn.2018.10.001

[2] WEATHERS SP, GILBERT MR. Advances in treating glioblastoma. F1000Prime Rep 2014; 6: 46. https://doi.org/10.12703/P6-46

[3] LAH TT, NOVAK M, BREZNIK B. Brain malignancies: Glioblastoma and brain metastases. Semin Cancer Biol 2020; 60: 262–273. https://doi.org/10.1016/j.semcancer.2019.10.010

[4] BROOKS LJ, CLEMENTS MP, BURDEN JJ, KOCHER D, RICHARDS L et al. The white matter is a pro-differentiative niche for glioblastoma. Nat Commun 2021; 12: 2184. https://doi.org/10.1038/s41467-021-22225-w

[5] VEHLOW A, CORDES N. Invasion as target for therapy of glioblastoma multiforme. Biochim Biophys Acta 2013; 1836: 236–244. https://doi.org/10.1016/j.bbcan.2013.07.001

[6] CUDDAPAH VA, ROBEL S, WATKINS S, SONTHEIMER H. A neurocentric perspective on glioma invasion. Nat Rev Neurosci 2014; 15: 455–465. https://doi.org/10.1038/nrn3765

[7] CHEN X, CUBILLOS-RUIZ JR. Endoplasmic reticulum stress signals in the tumour and its microenvironment. Nat Rev Cancer 2021; 21: 71–88. https://doi.org/10.1038/s41568-020-00312-2

[8] OAKES SA. Endoplasmic Reticulum Stress Signaling in Cancer Cells. Am J Pathol 2020; 190: 934–946. https://doi.org/10.1016/j.ajpath.2020.01.010

[9] BARTOSZEWSKA S, COLLAWN JF, BARTOSZEWSKI R. The Role of the Hypoxia-Related Unfolded Protein Response (UPR) in the Tumor Microenvironment. Cancers (Basel) 2022; 14: 4870. https://doi.org/10.3390/cancers14194870

[10] MADDEN E, LOGUE SE, HEALY SJ, MANIE S, SAMALI A. The role of the unfolded protein response in cancer progression: From oncogenesis to chemoresistance. Biol Cell 2019; 111: 1–17. https://doi.org/10.1111/boc.201800050

[11] ALMANZA A, CARLESSO A, CHINTHA C, CREEDICAN S, DOULTSINOS D et al. Endoplasmic reticulum stress signalling – from basic mechanisms to clinical applications. FEBS J 2019; 286: 241–278. https://doi.org/10.1111/febs.14608

[12] YOSHIDA H, OKADA T, HAZE K. ATF6 activated by proteolysis binds in the presence of NF-Y (CBF) directly to the cis-acting element responsible for the mammalian unfolded protein response. Mol Cell Biol 2000; 20: 6755–6767. https://doi.org/10.1128/MCB.20.18.6755-6767.2000

[13] HARDING HP, ZHANG Y, BERTOLOTTI A, ZENG H, RON D. Perk is essential for translational regulation and cell survival during the unfolded protein response. Mol Cell 2000; 5: 897–904. https://doi.org/10.1016/s1097-2765(00)80330-5

[14] KANEKO M, YASUI S, NIINUMA Y, OMURA T, OKUMA Y et al. A different pathway in the endoplasmic reticulum stress-induced expression of human HRD1 and SEL1 genes. FEBS Lett 2007; 581: 5355–5360. https://doi.org/10.1016/j.febslet.2007.10.033

[15] DIBDIAKOVA K, SAKSONOVA S, PILCHOVA I, KLACANOVA K, TATARKOVA Z et al. Both thapsigargin- and tunicamycin-induced endoplasmic reticulum stress increases expression of Hrd1 in IRE1-dependent fashion. Neurol Res 2019; 41: 177–188. https://doi.org/10.1080/01616412.2018.1547856

[16] LEE AH, IWAKOSHI NN, GLIMCHER LH. XBP-1 regulates a subset of endoplasmic reticulum resident chaperone genes in the unfolded protein response. Mol Cell Biol 2003; 23: 7448–7459. https://doi.org/10.1128/MCB.23.21.7448-7459.2003

[17] HAMPTON RY, SOMMER T. Finding the will and the way of ERAD substrate retrotranslocation. Curr Opin Cell Biol 2012; 24: 460–466. https://doi.org/10.1016/j.ceb.2012.05.010

[18] CHRISTIANSON JC, JAROSCH E, SOMMER T. Mechanisms of substrate processing during ER-associated protein degradation. Nat Rev Mol Cell Biol 2023; 24: 777–796. https://doi.org/10.1038/s41580-023-00633-8

[19] KIKKERT M, DOOLMAN R, DAI M, AVNER R, HASSINK G et al. Human HRD1 is an E3 ubiquitin ligase involved in degradation of proteins from the endoplasmic reticulum. J Biol Chem 2004; 279: 3525–3534. https://doi.org/10.1074/jbc.M307453200

[20] PRESTON GM, BRODSKY JL. The evolving role of ubiquitin modification in endoplasmic reticulum-associated degradation. Biochem J 2017; 474: 445–469. https://doi.org/10.1042/BCJ20160582

[21] HOLLIEN J, LIN JH, LI H, STEVENS N, WALTER P et al. Regulated Ire1-dependent decay of messenger RNAs in mammalian cells. J Cell Biol 2009; 186: 323–331. https://doi.org/10.1083/jcb.200903014

[22] HANAHAN D, WEINBERG RA. Hallmarks of cancer: the next generation. Cell 2011; 144: 646–674. https://doi.org/10.1016/j.cell.2011.02.013

[23] MARCINIAK SJ, CHAMBERS JE, RON D. Pharmacological targeting of endoplasmic reticulum stress in disease. Nat Rev Drug Discov 2022; 212: 115–140. https://doi.org/10.1038/s41573-021-00320-3

[24] KARAMALI N, EBRAHIMNEZHAD S, KHALEGHI MOGHADAM R, DANESHFAR N, REZAIEMANESH A. HRD1 in human malignant neoplasms: Molecular mechanisms and novel therapeutic strategy for cancer. Life Sci 2022; 301: 120620. https://doi.org/10.1016/j.lfs.2022.120620

[25] WANG Q, MORA-JENSEN H, WENIGER MA, PEREZ-GALAN P, WOLFORD C et al. ERAD inhibitors integrate ER stress with an epigenetic mechanism to activate BH3-only protein NOXA in cancer cells. Proc Natl Acad Sci U S A 2009; 106: 2200–2205. https://doi.org/10.1073/pnas.0807611106

[26] BREM GJ, MYLONAS I, BRÜNING A. Eeyarestatin causes cervical cancer cell sensitization to bortezomib treatment by augmenting ER stress and CHOP expression. Gynecol Oncol 2013; 128: 383–390. https://doi.org/10.1016/j.ygyno.2012.10.021

[27] WANG X, CHEN JX, LIU YH, YOU C, MAO Q. Mutant TP53 enhances the resistance of glioblastoma cells to temozolomide by up-regulating O(6)-methylguanine DNA-methyltransferase. Neurol Sci 2013; 34: 1421–1428. https://doi.org/10.1007/s10072-012-1257-9

[28] LIN LL, WANG HH, PEDERSON B, WEI X, TORRES M et al. SEL1L-HRD1 interaction is required to form a functional HRD1 ERAD complex. Nat Commun 2024; 17: 1440. https://doi.org/10.1038/s41467-024-45633-0

[29] FUJITA H, YAGISHITA N, ARATANI S, SAITO-FUJITA T, MOROTA S, et al. The E3 ligase synoviolin controls body weight and mitochondrial biogenesis through negative regulation of PGC-1β. EMBO J 2015; 34: 1042–1055. https://doi.org/10.15252/embj.201489897.

[30] ZHOU Z, TORRES M, SHA H, HALBROOK CJ, VAN DEN BERGH F et al. Endoplasmic reticulum-associated degradation regulates mitochondrial dynamics in brown adipocytes. Science 2020; 368: 54–60. https://doi.org/10.1126/science.aay2494

[31] FIORESE CJ, SCHULZ AM, LIN YF, ROSIN N, PELLEGRINO MW et al. 2016 The Transcription Factor ATF5 Mediates a Mammalian Mitochondrial UPR. Curr Biol 2016; 26: 2037–2043. https://doi.org/10.1016/j.cub.2016.06.002

[32] BRODNANOVA M, HATOKOVA Z, EVINOVA A, CIBULKA M, RACAY P. Differential impact of imipramine on thapsigargin- and tunicamycin-induced endoplasmic reticulum stress and mitochondrial dysfunction in neuroblastoma SH-SY5Y cells. Eur J Pharmacol 2021; 902: 174073. https://doi.org/10.1016/j.ejphar.2021.174073

[33] YAMASAKI S, YAGISHITA N, SASAKI T, NAKAZAWA M, KATO Y et al. Cytoplasmic destruction of p53 by the endoplasmic reticulum-resident ubiquitin ligase 'Synoviolin'. EMBO J 2007; 26: 113–122. https://doi.org/10.1038/sj.emboj.7601490

[34] YAGISHITA N, ARATANI S, LEACH C, AMANO T, YAMANO Y et al. RING-finger type E3 ubiquitin ligase inhibitors as novel candidates for the treatment of rheumatoid arthritis. Int J Mol Med 2012; 30: 1281–286. https://doi.org/10.3892/ijmm.2012.1129

[35] JI Y, LUO Y, WU Y, ZHAO L, XUE Z et al. SEL1L-HRD1 endoplasmic reticulum-associated degradation controls STING-mediated innate immunity by limiting the size of the activable STING pool. Nat Cell Biol 2023; 25: 726–739. https://doi.org/10.1038/s41556-023-01138-4

[36] LUO S, BAUMEISTER P, YANG S. ABCOUWER SF, LEE AS. Induction of Grp78/BiP by translational block: activation of the Grp78 promoter by ATF4 through and upstream ATF/CRE site independent of the endoplasmic reticulum stress elements. J Biol Chem 2003; 278: 37375–37385. https://doi.org/10.1074/jbc.M303619200

[37] LIU K, TSUNG K, ATTENELLO FJ. Characterizing Cell Stress and GRP78 in Glioma to Enhance Tumor Treatment. Front Oncol 2020; 10: 608911. https://doi.org/10.3389/fonc.2020.608911

[38] OMURA T, MATSUDA H, NOMURA L, IMAI S, DENDA M et al. Ubiquitin ligase HMG-CoA reductase degradation 1 (HRD1) prevents cell death in a cellular model of Parkinson's disease. Biochem Biophys Res Commun 2018; 506: 516–521. https://doi.org/10.1016/j.bbrc.2018.10.094

[39] LEE A. Glucose-regulated proteins in cancer: molecular mechanisms and therapeutic potential. Nat Rev Cancer 2014; 14: 263–276. https://doi.org/10.1038/nrc3701

https://doi.org/10.4149/neo_2025_241120N481

Inhibition of enzymatic activity of HRD1 results in death of cells derived from glioblastoma multiforme, neuroblastoma, and normal astrocytes

Jaroslava GUZIKOVA[1], Monika LISKOVA[1], Lubos HUDAK[1], Maria BRODNANOVA[2], Andrea EVINOVA[2], Jozef HATOK[1], Peter RACAY[1,*]

Supplementary Information

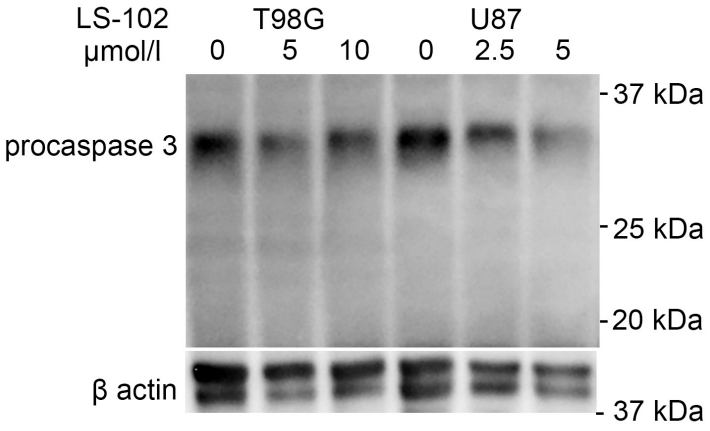

Supplementary Figure S1. Impact of LS-102 on caspase3 expression in glioblastoma cells. Total cell extracts were prepared from T98G and U87 cells after treatment with indicated concentrations of LS-102. The effect of the treatment on the level of caspase3 was evaluated by Western blot analysis of total cell extracts as described in Materials and methods. β-actin served as the loading control. The representative blots are cropped from different parts of the same blot.